A mechanistic analysis of the influence of iron-oxidizing bacteria on antimony (V) removal from water by microscale zero-valent iron

Li, Yongchao; Wu, Jixin; Ren, Bozhi; Hursthouse, Andrew

Published in:
Journal of Chemical Technology and Biotechnology

DOI:
10.1002/jctb.5606

E-pub ahead of print: 09/02/2018

Document Version
Peer reviewed version

A mechanistic analysis of the influence of iron-oxidizing bacteria on antimony (V) removal from water by microscale zero-valent iron

Li Yongchao [1] *, Wu Jixin [1], Hu Wei [2], Ren Bozhi [3], Hursthouse S. Andrew [1,3,4]

[1]School of Civil Engineering, Hunan University of Science and Technology, Xiangtan 411201, China;

[2]School of Life Sciences, Hunan University of Science and Technology, Xiangtan 411201, China;

[3]Hunan Provincial Key Laboratory of Shale Gas Resource Utilization, Xiangtan 411201, China;

[4]School of Science and Sport, University of the West of Scotland, Paisley PA1 2BE, UK

Abstract

BACKGROUND: Microscale zero-valent iron (mZVI) is an efficient material for removing heavy metals from water, and iron-oxidizing bacteria are the primary microorganisms responsible for iron corrosion. We investigated the effects of *Sphaerotilus natans* on antimony [Sb(V)] removal by mZVI using batch experiments.

RESULTS: At an initial Fe^0 dose of $0.1 g \cdot L^{-1}$, 40 $mg \cdot L^{-1}$ Sb(V) was almost completely removed in an abiotic system. Although *Sphaerotilus natans* exhibited significant tolerance to Sb(V), its ability to adsorb Sb(V) was poor. Most importantly, the presence of *Sphaerotilus natans* reduced the removal rate of aqueous Sb(V) by mZVI by up to 39%. The value of the redox potential in the biologically mediated system was lower than that in the abiotic control, indicating oxygen consumption by *Sphaerotilus natans*. In the presence of *Sphaerotilus natans*, the main reaction products were FeOOH and

This article has been accepted for publication and undergone full peer review but has not been through the copyediting, typesetting, pagination and proofreading process, which may lead to differences between this version and the Version of Record. Please cite this article as doi: 10.1002/jctb.5606

$FeSb_2O_6$, compared to Fe_2O_3 in the abiotic system. Biomineralization of Fe^{3+} ions by *Sphaerotilus natans* may have occurred during the experiment, but it did not play a significant role in Sb(V) removal.

CONCLUSION: mZVI can be efficiently used to remove Sb(V) from water. However, the presence of *Sphaerotilus natans* may inhibit its removal ability, likely due to the decreased mass transfer and lower corrosion of iron.

Keywords: antimony (V); microscale zero-valent iron; iron-oxidizing bacteria; bioinhibitory effect

INTRODUCTION

Antimony (Sb) is a metalloid in Group VA of the periodic table, and the Sb(III) and Sb(V) oxidation states are the most prevalent in the environment.[1] Sb and its compounds are hazardous to human health, with significant carcinogenicity, and Sb(III) is more toxic than Sb(V).[2] Antimony and its compounds are considered priority pollutants by the Council of the European Communities[3] and by the United States Environmental Protection Agency.[4] The World Health Organization requires that the maximum level of Sb in drinking water be less than 20 μg L^{-1}.[5]

Most Sb gets into the environment from anthropogenic sources such as soil runoff, road traffic emissions, fossil fuel combustion, mining, and smelting activities.[6, 7] The mining industry in particular produces a great quantity of mine drainage and waste residue, which can have significant impacts on the local environment. For example, due to the historic mining activities in the Kantishna Hills mining district of interior Alaska,

Sb and arsenic concentrations in nearby watersheds were as high as 0.72 $mg \cdot L^{-1}$ and 0.239 $mg \cdot L^{-1}$, respectively.[8] Because improperly treated mining and smelting wastewater was discharged into the environment, dissolved Sb concentrations in streams ranged from 4.58 to 29.4 $mg \cdot L^{-1}$ in the Xikuangshan Sb mining area of China,[9] levels that pose high health risks to the public. Consequently, different methods for treating antimony-contaminated water have recently been developed.

Adsorption is one of the most effective techniques for the removal of Sb from aqueous solution owing to its high efficiency, simplicity, and rapid response.[10, 11] Commonly used adsorbents for Sb include nanomaterials, activated carbon, bentonite, and iron-based oxides and residues.[12, 13] However, most of these materials are produced through complicated chemical methods or require modifications, and thus the treatment costs for significant quantities of Sb-containing wastewater are high. Available zero-valent iron (ZVI) has been shown to be an efficient and cost-effective material for removing heavy metals, nitrates, hydrocarbons from water.[14–16] Under aerobic conditions, Fe^0 is oxidized by O_2 in water, yielding Fe^{2+} ions. The resulting Fe^{2+} can be further oxidized to Fe^{3+} ions, and then hydrolyzed to form iron oxide precipitates. The contaminants are therefore trapped within the precipitates and removed from the water.[17] Sb(V) in model solution can be immobilized by ZVI, and a maximum of 18.1 mg $Sb(V) \cdot g^{-1}$ ZVI has been achieved. The incorporation of Sb(V) into the structure of iron (hydr)oxides has been evaluated using X-ray absorption fine structure spectroscopy analysis.[18] The influence of tartrate and a weak magnetic field on the removal of Sb(III)

by ZVI has also been investigated with batch and semi-continuous reactors.[19] Nanoscale zero-valent iron (nZVI) has also drawn attention as an effective approach for removing Sb from solution.[20, 21] The influence of a range of processing parameters on Sb removal by Fe^0 has been systematically investigated, including contact time, solution pH, initial Sb concentration, co-existing ions, and the effects of weak magnetic fields. In addition to these physical and chemical factors, the high abundance of microorganisms in the aqueous environment may significantly influence the performance of ZVI in water treatment systems. Microorganisms can attach to iron surfaces and cause microbiologically influenced corrosion.[22] Furukawa *et al*.[23] and Wilkin *et al*.[24] demonstrated that some iron corrosion products, including iron hydroxides, oxy-hydroxides, and green rusts, are beneficial in arsenic removal from water. Nonetheless, An *et al*.[25] reported that the presence of hydrogenotrophic bacteria in water generated a lepidocrocite layer on iron surfaces and decreased the nitrate removal rate of nZVI. The influence of microorganismal activity on the removal of Sb by ZVI remains unclear.

Aerobic iron-oxidizing bacteria (IOB) constitute one of the major iron corrosion pathways in surface environments. They attach to the surface of iron-rich materials and generate biological iron oxide minerals.[26, 27] In an aerobic environment, IOB can oxidize ferrous ions and deposit iron hydroxides extracellularly.[28] *Sphaerotilus natans*, which belongs to the IOB consortia, exists naturally in ecological communities found in heavily polluted freshwater and activated sludge systems in the form of superficial

mucilage layers.[29, 30] Starosvetsky *et al*.[31] isolated IOB from rust deposits on a clogged carbon steel heat exchanger in Israel, and the primary strain was also identified as a *Sphaerotilus* sp. In addition, living and lyophilized *Sphaerotilus natans* can be used to treat heavy metal cations by biosorption.[32] When considering the potential of ZVI in the treatment of Sb-contaminated wastewater, the impacts of biofilms in the treatment system on long-term performance must be considered. There is little previously published information on the removal of Sb from water by ZVI in the presence of microorganisms, especially *Sphaerotilus natans*.

Sb(V) is the dominant form of Sb in water at most environmentally relevant pH levels; [1] therefore, it was selected as the target pollutant in this study. The main objectives of this paper were to (1) investigate Sb(V) removal by microscale zero-valent iron (mZVI) in abiotic systems; (2) assess the Sb(V) adsorption ability of *Sphaerotilus natans* and its biomineralization; (3) study the Sb(V) removal ability of ZVI in the presence of *Sphaerotilus natans*; and (4) explore the mechanism of the bioinhibitory effect of *Sphaerotilus natans* on Sb(V) remediation with ZVI.

MATERIALS AND METHODS

Cultivation of microorganisms

In this study, lyophilized *Sphaerotilus natans* NBRC#13543 was purchased from Beijing Yuding Xinjie Technology, Ltd. (Beijing, China). The cultivation medium contained polypeptone (10 $g \cdot L^{-1}$), yeast powder (2 $g \cdot L^{-1}$), agar (15 $g \cdot L^{-1}$), magnesium sulfate heptahydrate (1 $g \cdot L^{-1}$), and ammonium iron citrate (10 $mg \cdot L^{-1}$). The culture

medium was autoclaved at 121°C for 20 min after the initial pH was adjusted to 7.0. After cultivation for two consecutive generations, the strain grew normally. Colonies on plates were sampled with a sterile loop, inoculated in 250-mL conical flasks containing liquid culture medium, and then incubated at 30°C. The biomass growth was monitored by measuring the optical density (OD), and the growth curve of *Sphaerotilus natans* was investigated.

Effects of dissolved oxygen (DO) and pH on Sb(V) removal by ZVI in abiotic systems

An Sb(V) stock solution with an Sb concentration of 500 $mg \cdot L^{-1}$ was prepared by dissolving $KSb(OH)_6$ in 2 $mol \cdot L^{-1}$ HCl solution. Experimental solutions of Sb(V) were obtained by diluting the stock solution with deionized (DI) water. mZVI was first added to a conical flask containing 200 mL of 40 $mg \cdot L^{-1}$ Sb(V) solution and then covered with a ventilated rubber stopper. All flasks were placed on a rotary shaker at 100 $r \cdot min^{-1}$ at 30°C. At timed intervals, samples were taken from the suspension, filtered through 0.45-μm membrane filters, and analyzed for total Sb remaining in the aqueous phase. Additionally, the redox potential (Eh) of the solution was monitored as the reaction progressed.

To test the effects of dissolved oxygen (DO) on Sb(V) removal, a fixed amount of mZVI was added to serum bottles after the initial Sb(V) solution was purged with N_2 gas for 2 h. Then, the bottles were sealed with Teflon septa and aluminum crimps, followed by mixing at 100 $r \cdot min^{-1}$ on a rotary shaker at 30°C. At timed intervals, the Sb

concentration in the solution was determined as above. The normalized residual concentration (C/C_0) was used to describe the removal kinetics.

To test the effects of solution pH on Sb(V) adsorption, the initial pH of Sb(V) solutions was pre-adjusted to 5.0, 6.0, 7.0, and 8.0 with 1.0 mol·L^{-1} HCl or 1.25 mol·L^{-1} NaOH. Then, mZVI was added, and the conical flasks were covered with ventilated rubber stoppers. The analysis of residual Sb during the process was as described above.

Sb(V) adsorption tests with *Sphaerotilus natans* biomass

After cultivation in liquid culture medium for 12 h, 5 mL of *Sphaerotilus natans* suspension was added to 250-mL conical flasks containing 195 mL Sb(V) solution. The initial solution pH was 7.0, and the Sb(V) concentration was 40 mg·L^{-1}. The flasks were placed on a rotary mixer at 30°C. The OD at 500 nm (OD_{500}) and residual Sb(V) concentrations in solution were monitored during the subsequent reaction.

Sb(V) removal ability of mZVI in the presence of *Sphaerotilus natans*

Aliquots (5, 10, 15, and 20 mL) of *Sphaerotilus natans* cell suspension (1.6×10^9 CFU mL^{-1}) that were cultivated for 12 h and 0.02 g ZVI were added to flasks containing an aqueous solution of Sb(V) without nutrients. The initial Sb(V) concentration in all flasks was approximately 40 mg·L^{-1}, and the initial pH was 7.0. The flasks were covered with ventilated rubber stoppers and placed on a rotary shaker at 100 r·min^{-1} at 30°C. *Sphaerotilus natans* biomass, residual Sb(V) concentration, and Eh value in solution were analyzed as the reaction progressed. After the reaction, the morphologies and main chemicals of the precipitates were analyzed.

Characterization

The particle size and morphology of fresh mZVI and generated products were examined using scanning electron microscopy (SEM, JSM-6380LV, JEOL, Japan). The chemical composition and crystal structures of the precipitates after reaction were characterized using X-ray diffraction (XRD, D8 Advance, Bruker, Germany). Functional groups on the surface of samples were measured by Fourier transform infrared spectrometry (FTIR, Nicolet 6700, USA) using the standard KBr disk method. *Sphaerotilus natans* in suspension was imaged by high resolution scanning electron microscopy (HRSEM, SU8010, Hitachi, Japan).

Analytical methods

Total Sb in solution was analyzed using a flame atomic absorption spectrophotometer (AA-7001, East & West Analytical Instruments, Inc., Beijing), with suitable matrix-matched standards and replicates. The Eh value of the solution was determined using a BPP-920 ORP meter (BELL Analytical Instruments Co., Ltd., Dalian, China). The pH values were measured using a basic PB-10 meter (Sartorius, Germany). The number of colony-forming units (CFU) in the solution was determined by surface plating at appropriate dilutions.[33] All experiments were carried out in triplicate, and the averages are reported.

RESULTS AND DISCUSSION

Removal of Sb(V) by mZVI in abiotic systems

Effects of DO on Sb(V) removal by ZVI

Oxygen is a major electron acceptor in reduction systems, and it plays a complicated role in the mZVI reaction. The presence of O_2 in the iron–water system has been shown to increase the reduction of monochloroacetic and dichloroacetic acid, and to decrease the removal efficiency of bromate and nitrate.[34] However, investigations of the effects of O_2 on $Sb(OH)_6^-$ removal have been limited.

The removal of Sb(V) from water solution using mZVI without N_2 purging is shown in Fig. 1a. At initial doses of 0.05, 0.1, 0.15, and 0.25 $g \cdot L^{-1}$ Fe, a total of 76.2, 90.6, 95.7 and 100% of 40 $mg \cdot L^{-1}$ Sb(V) were removed within 24 h, respectively. The removal rates then gradually increased, finally reaching 84.6, 99, 100, and 100%, respectively. Increasing the amount of mZVI resulted in faster and more extensive removal of Sb(V) from the aqueous phase, mainly because the increased dose of Fe would increase the total surface area and thus the available active sites for Sb(V) sorption.[35] The Eh value in solution was examined during the experiment, as shown in Fig. 1b. It decreased sharply from 421–497 mV to 99–150 mV after 12 h, followed by a slow increase, reaching 150–320 mV at the end of the experiment. DO depletion may be an important reason for this Eh decrease in solution. Li *et al.*[18] suggested that the main mechanism for Sb(V) removal by ZVI was the incorporation of Sb(V) into the structure of iron (hydr)oxides from iron corrosion. The Fe^0 in water was oxidized by O_2, producing Fe^{2+}, which can be subsequently oxidized to Fe^{3+} and generate iron oxides. Therefore, much of the O_2 was consumed as result of iron corrosion, according to Eqs. (1–3):[17, 36]

$$Fe^0 + H_2O + 1/2\ O_2 \rightarrow Fe^{2+} + 2OH^- \quad (1)$$

$$Fe^{2+} + 1/2\ H_2O + 1/4\ O_2 \rightarrow Fe^{3+} + OH^- \quad (2)$$

$$Fe^{3+} + 3H_2O \rightarrow Fe(OH)_3 + 3H^+. \quad (3)$$

In addition, ZVI (Fe^{2+}/Fe^0), with a standard reduction potential of −0.44 V,[37] can reduce any species with a potential lower than that of Fe. The primary Sb(V) species, ($Sb(OH)_6^-$), has a standard electric potential of +0.76 V,[38] and the overall electrochemical reaction is thermodynamically favorable. Dorjee *et al.*[20] demonstrated that a fraction of the Sb(V) species was reduced to Sb(III) when Sb(V) was chemisorbed and interacted with the "FeOOH" layer on the nZVI surface. Although the reduction rate of mZVI was not as fast as that of nZVI, the reduction of Sb(V) by mZVI to Sb(III) species may have occurred. In general, as the reduction and precipitate reaction progressed, the Eh value decreased.[39, 40] After 24 h, the Sb(V) removal reaction slowed, and the Eh values in solution increased again, which was thought to be due to the increase in DO in solution owing to O_2 diffusion.

After the Sb(V) solution was purged with N_2, the dynamic process of Sb(V) removal with mZVI was studied. As shown in Fig. 2, at the initial Fe doses of 0.05, 0.1, 0.15, and 0.25 $g \cdot L^{-1}$, 78, 83, 84.9, and 93.2% of Sb(V) was removed by mZVI after 96 h of the reaction process, respectively. The Sb(V) removal rate by mZVI was reduced by 6.6–16%. This was likely due to the absence of soluble Fe^{2+}, which is normally produced by the anaerobic corrosion of Fe^0, according to Eq. (4)[36]:

$$Fe^0 + 2H_2O \rightarrow Fe^{2+} + H_2 + 2OH^- \quad (4)$$

Thus, the formation of iron oxides, which can more effectively adsorb Sb(V), cannot occur unless there is enough O_2 in the water. This is similar to aqueous Cr(VI) removal kinetics in that mZVI was found to be greater under oxic than under anoxic conditions due to the formation of iron oxides, even though Cr(VI) was reduced to Cr(III) by Fe^0 under both conditions.[41] Overall, the presence of DO in solution has a significant benefit for the removal of Sb(V) by mZVI.

Effects of solution pH on Sb(V) removal

We next investigated the influence of pH on the removal of Sb(V) by mZVI under aerated conditions. As shown in Fig. 3a, 100, 100, 99, and 89.79% of 40 $mg \cdot L^{-1}$ Sb(V) was removed by 0.1 $g \cdot L^{-1}$ mZVI at the initial pH levels of 5.0, 6.0, 7.0, and 8.0, respectively. The pH slowly increased as the reaction progressed, although no acid or alkali was added to maintain the pH throughout the process. After 96 h, the final pH ranged from 7.45 to 8.81 (Fig. 3b). Thus, the removal of Sb(V) by mZVI was more effective at lower pH values. This was because decreased pH accelerated the corrosion of iron and the generation of iron oxides. As the conditions of Sb mine drainage in China fall within the weak acid to weak base pH range, subsequent tests of Sb(V) removal were carried out at a pH of 7.0.

Adsorption of Sb(V) by *Sphaerotilus natans* biomass

Growth tests of *Sphaerotilus natans*

Preliminary tests were carried out to study the growth behavior of *Sphaerotilus natans* in liquid culture medium at different initial pH values. The fastest growth was obtained

at an initial pH of 7.0, and the growth of the strain was poor when the pH was below 6.0 (Fig. S1). Solisio *et al*.[29] suggested that the growth of *Sphaerotilus natans* cells was negligible below pH 6.0. The lag phase of biomass growth lasted for less than 6 h. Once they adapted to culture medium with an initial pH of 7.0, the cells grew rapidly, and the maximum OD_{500} reached 1.41 after 36 days of cultivation.

Bioadsorption of Sb(V) by *Sphaerotilus natans* from solution

After 5 mL of cell suspension was added to Sb(V) solution, we investigated the ability of *Sphaerotilus natans* to bioadsorb during culture growth. As shown in Fig. 4, the initial OD_{500} of the solution was 1.09. It deceased to 0.94 after 6 h as a result of the adaptation of the bacteria, and gradually increased during the next treatment. Therefore, *Sphaerotilus natans* exhibited significant tolerance to Sb(V). Although there was some fluctuation, the removal rate of Sb(V) was only 5.4% at the end of experiment. It has been previously demonstrated that *Sphaerotilus natans* efficiently adsorbs Cu^{2+} and Cd^{2+} ions.[42] Qin *et al*.[43] showed that electrostatic attraction played a major role in the sorption process, despite the presence of active $–CONH_2$ and –OH groups on the cell surface. In our study, *Sphaerotilus natans* showed low adsorption capacity toward Sb(V), which may have been due to weak electrostatic attraction between $Sb(OH)_6^-$ and the negatively charged microorganisms.[44]

Sb(V) removal from water by mZVI in the presence of *Sphaerotilus natans*

Fig. 5 shows the influence of *Sphaerotilus natans* on Sb(V) removal by mZVI and the corresponding total number of CFU and Eh values in a solution with an initial pH of 7.0.

As shown in Fig. 5a, with additions of 5, 10, 15, and 20 mL of biomass, the final Sb(V) removal rates were approximately 85.4, 71.7, 62.4, and 60.3%, respectively. Under identical reaction conditions, the removal rate of Sb(V) by mZVI in the absence of *Sphaerotilus natans* was approximately 99%. Thus, the removal of Sb(V) decreased by 13.6–38.7% upon the addition of the *Sphaerotilus natans* suspension. Previous experiments have indicated that *Sphaerotilus natans* alone has little capacity to adsorb Sb(V). Thus, the presence of *Sphaerotilus natans* seriously inhibited the removal efficiency of Sb(V) by mZVI. Moreover, the removal of Sb(V) decreased when the initial biomass increased. This likely occurred because a large mass of *Sphaerotilus natans* would decrease the exposure of the iron surface area, negatively affecting mass transfer. The previous experiment also indicated that moderate DO was important for Sb(V) removal by mZVI and that the DO was likely to decrease as O_2 was consumed by aerobic *Sphaerotilus natans*.

The total number of bacterial colonies was monitored during the experiment to assess the growth rate of *Sphaerotilus natans* in the presence of mZVI. As shown in Fig. 5b, the total number of CFUs in solution ranged from 0.38 to 1.5×10^8 CFU mL^{-1} after the addition of *Sphaerotilus natans*, and then increased to $0.9–4.0 \times 10^8$ CFU mL^{-1} after cultivation for 12 h. Because *Sphaerotilus natans* is an oligotrophic bacterium and due to its strong tolerance to Sb(V), its adaptive phase was relatively short. After 24 h, the cells were nearly in the stationary growth phase. The total number of CFUs in solution with the initial addition of 20 mL of biomass was greater than that in solutions with

initial additions of 5, 10, and 15 mL of biomass. Meanwhile, the number of cells in the Sb(V) solution containing 5 mL of biomass decreased rapidly due to insufficient nutrients. After 24 h of rapid growth of *Sphaerotilus natans*, the corresponding Eh value in solution was greatly reduced as a result of the high consumption of the limited O_2.[45] It ultimately declined to approximately 10–52 mV (Fig. 5c), much lower than the Eh value of the abiotic solution.

Mechanism analysis

SEM characterization of the products from abiotic and biotic systems

Fresh mZVI (Fig. 6a) before a reaction had an irregular spherical shape with a smooth surface, and a diameter ranging from 10 to 40 μm. However, after reaction with Sb(V) solution without purging N_2, the product in the abiotic system (Fig. 6b) was not uniform in size, and many small particulates with rough surfaces were formed. In the presence of 10 mL *Sphaerotilus natans*, the product surface recovered and exhibited a clustered shape (Fig. 6c and d) in the biologically mediated system, indicating that different products may have been generated in these two systems.

XRD characterization of products after reaction

Powder XRD was used to further investigate the differences between the products generated in the biological and abiotic reaction systems. As presented in Fig. 7a, solid products in the abiotic reaction system without N_2 purging exhibited broad diffraction peaks at approximately 32, 41.5, 54, and 63.5°, a feature of amorphous Fe_2O_3.[46] No diffraction peaks for Sb-specific phases were detected in the product, as this was likely

to be at low levels and may have been non-crystalline or sorbed into other phases. Compared with the abiotic reaction system, the amorphous Fe_2O_3 pattern of the product in the biological reaction systems was much weaker. However, the potential presence of FeOOH was indicated by the diffraction peaks at 2θ values of 36.6 and 53.2°.[47, 48] Strong diffraction peaks were observed at 43.1 and 81.5°, which was identified as $FeSb_2O_6$ with JCPDS Card No. 07-0349. The presence of Fe(II) in $FeSb_2O_6$ was probably due to the growth of *Sphaerotilus natans* resulting in insufficient O_2 and inhibiting the oxidization of ferrous ions. In addition, the characteristic diffraction peaks of Fe^0 were not observed, probably because the surface of mZVI was covered by a thick layer of precipitate.

FTIR characterization of the products

After reaction with Sb(V) solution, the product was also characterized by FTIR. As shown in Fig. 8, the absorption peaks observed at approximately 3300 cm^{-1} and 1640 cm^{-1} in all three samples were assigned to the bond stretching of O–H and the bending vibration of adsorbed water, respectively.[49] The broad peak ranging from 700 to 400 cm^{-1} observed in all samples may be assigned to the Fe–O bond of iron oxides or Sb–O bending vibrations,[21] indicating the presence of interactions between Fe–O bonds with Sb(V). In the FTIR spectrum of the product in the biological system, the peak appearing at 1540 cm^{-1} was closely related to the N–H from proteins, and the peak at 1380 cm^{-1} may be attributed to the C–H bending vibrations, suggesting the presence of biomass.[50]

Characterization of *Sphaerotilus natans* in suspension after reaction

At the end of the experiment, the suspension that contained the biomass was collected and characterized with HRSEM (Fig. 9a and b). After cultivation in Sb(V) solution for 96 h, the cells still maintained a short rod shape. There were some small deposits near the bacteria, and also larger porous flocs that covered several cells. Aside from *Leptothrix*, *Crenothrix*, *Clonothrix*, and *Hyphomicrobium* sp., *Sphaerotilus* sp. is one of the best-documented examples of IOB in aquatic systems, which can bind and precipitate ferric iron non-specifically onto their cell surfaces to form precipitates.[31, 51] Sun[52] found that the mineralization and crystallization of $Fe(OH)_3$ gel occurred both inside and outside *Sphaerotilus* sp. cells in a solution containing 0.01 mol·L^{-1} Fe^{3+}. The main product was weak crystalline akaganeite (β-FeOOH) nanoparticles. Moreover, the naturally biomineralized iron oxides had a strong adsorptive capacity to Cr(VI). The morphology and structure of iron (hydr)oxides formed through the mineralization of $Fe(OH)_3$ gel varied with the ingredients and concentrations of organic matrices.

During the reaction with Sb(V) solution, the corrosion of mZVI produced Fe^{3+} ions that were precipitated by *Sphaerotilus natans*. This is supported by the XRD data, which demonstrated the generation of FeOOH in the presence of *Sphaerotilus natans* in solution. Therefore, we can conclude that biomineralization of *Sphaerotilus natans* actually occurred in the experiment. Although different kinds of iron oxides or hydroxides have recently been widely used to remove Sb from water,[13] the Sb(V) removal ability of mZVI was seriously reduced in the presence of *Sphaerotilus natans*, indicating that the adsorption ability of biologically formed iron oxides did not play a

major role in Sb(V) removal.

CONCLUSIONS

ZVI has great potential in the environmental remediation of metal ions in water. However, the removal of Sb(V) by ZVI in the presence of microorganisms was not previously well understood. The effects of *Sphaerotilus natans* on Sb(V) removal by mZVI were investigated for the first time in this study. Our results indicated that although *Sphaerotilus natans* had some adsorption ability towards Sb(V), the presence of *Sphaerotilus natans* seriously inhibited the ability of mZVI to remove Sb(V), probably because the mass transfer and corrosion of iron were lowered. The biomineralization of Fe^{3+} ions by *Sphaerotilus natans* may have occurred during the experiment, but adsorption to biogenic minerals did not play a primary role in Sb(V) removal. The main product in the abiotic system was Fe_2O_3, whereas FeOOH and $FeSb_2O_6$ were produced in the presence of *Sphaerotilus natans*.

ACKNOWLEDGEMENTS

This work was supported by the National Nature Science Foundation of China (No. 51504094 and 31401943). Andrew S. Hursthouse acknowledges the support of Hunan Provincial Government and Hunan University of Science & Technology through the High End Expert Scholarship.

REFERENCES

1 Filella M, Belzile N, Chen YW, Antimony in the environment: A review focused on natural waters. II. Relevant solution chemistry. *Earth Sci Rev* **59**: 265–285 (2002).

2 Seiler HG, Sigel A, Sigel H, Handbook on metals in clinical and analytical chemistry. Marcel Dekker, New York (1994).

3 Council of the European Communities, Council Directive 76/464/EEC of 4 May 1976 on pollution caused by certain dangerous substances discharged into the aquatic environment of the community. *Official Journal L* **129**: 23–29 (1976).

4 United States Environmental Protection Agency, Water Related Fate of the 129 Priority Pollutants. Office of Water Planning and Standards. Washington, DC (1979).

5 WHO. Guidelines for drinking-water quality: volume 2. Health criteria and other supporting information 2nd ed, World Health Organization, Geneva (1996).

6 Filella M, Belzile N, Chen YW, Antimony in the environment: a review focused on natural waters I. Occurrence. *Earth-Science Rev* **57**: 125–176 (2002).

7 Li YC, Hu XX, Ren BZ, Treatment of antimony mine drainage: challenges and opportunities with special emphasis on mineral adsorption and sulfate reducing bacteria. *Water Sci Technol* **73**: 2039-2051 (2016).

8 Ritchie VJ, Ilgen AG, Mueller SH, Trainor TP, Goldfarb RJ, Mobility and chemical fate of antimony and arsenic in historic mining environments of the Kantishna Hills district, Denali National Park and Preserve, Alaska. *Chem Geol* **335**: 172–188 (2013).

9 He MC, Wang XQ, Wu FC, Fu ZY, Antimony pollution in China. *Sci Total Environ* **421**: 41–50 (2012).

10 Luo JM, Luo XB, Crittenden J, Qu JH, Bai YH, Peng Y, Li JH, Removal of antimonite (Sb(III)) and antimonate (Sb(V)) from aqueous solution using carbon nanofibers that are decorated with zirconium oxide (ZrO_2). *Environ Sci Technol* **49**: 11115–11124 (2015).

11 Yang WC, Tang QZ, Wei JM, Ran YJ, Chai LY, Wang HY, Enhanced removal of Cd(II) and Pb(II) by composites of mesoporouscarbon stabilized alumina. *Appl Surf Sci* **369**: 215–223 (2016).

12 Iqbal M, Saeed A, Edyvean RGJ, Bioremoval of antimony(III) from contaminated water using several plant wastes: optimization of batch and dynamic flow conditions for sorption by green bean husk (Vigna radiata). *Chem Eng J* **225**: 192–201 (2013).

13 Xu W, Liu RP, Qiu JH, Peng RM, Adsorption of antimony(V) onto Mn(II)-enriched surfaces of manganese oxide and Fe-Mn binary oxide. *Chemosphere* **138**: 616–624 (2015).

14 Guo XJ, Yang Z, Dong HY, Guan XH, Ren QD, Lv XF, Jin X, Simple combination of oxidants with zero-valent-iron (ZVI) achieved very rapid and highly efficient removal of heavy metals from water. *Water Res* **88**: 671–680 (2016).

15 Velasco A, Aburto-Medina A, Shahsavari E, Revah S, Ortiz I, Degradation mechanisms of DDX induced by the addition of toluene and glycerol as cosubstrates in a zero-valent iron pretreated soil. *J Hazard Mater* **321**: 681–689 (2017).

16 Song XJ, Chen ZH, Wang XM, Zhang SJ, Ligand effects on nitrate reduction by zero-valent iron: Role of surface complexation. *Water Res* **114**: 218–227 (2017).

17 Noubactep C, An analysis of the evolution of reactive species in Fe^0/H_2O systems. *J Hazard Mater* **168**: 1626–1631 (2009).

18 Li JL, Bao HL, Xiong XM, Sun YK, Guan XH, Effective Sb(V) immobilization from water by zero-valent iron with weak magnetic field. *Sep Purif Technol* **151**: 276–283 (2015).

19 Fan P, Sun Y, Qiao J, Lo IMC, Guan X, Influence of weak magnetic field and tartrate on the oxidation and sequestration of Sb(III) by zerovalent iron: Batch and semi-continuous flow study. *J Hazard Mater* **343**: 266-275 (2017).

20 Dorjee P, Amarasiriwardena D, Xing BS, Antimony adsorption by zero-valent iron nanoparticles (nZVI): Ion chromatography–inductively coupled plasma mass spectrometry (IC–ICP-MS) study. *Microchem J* **116**: 15–23 (2014).

21 Zhao XQ, Dou XM, Mohan D, Pittman CU, OK YS, Jin X, Antimonate and antimonite adsorption by a polyvinyl alcohol-stabilized granular adsorbent containing nanoscale zero-valent iron. *Chem Eng J* **6**: 4268–4274 (2014).

22 Liu HW, Fu CY, Gu TY, Zhang GA, Lv YL, Wang HT, Liu HF, Corrosion behavior of carbon steel in the presence of sulfate reducing bacteria and iron oxidizing bacteria cultured in oilfield produced water. *Corros Sci* **100**: 484–495 (2015).

23 Furukawa Y, Kim JW, Watkins J, Wilkin RT, Formation of ferrihydrite and associated iron corrosion products in permeable reactive barriers of zerovalent

iron. *Environ Sci Technol* **36**: 5469–5475 (2002).

24 Wilkin RT, Acree SD, Beak DG, Ross RR, Lee TR, Paul CJ, Field application of a permeable reactive barrier for treatment of arsenic in ground water. Report EPA 600/R-08/093, U.S. Environmental Protection Agency, Office of research and development, Washington, DC (2008).

25 An Y, Dong Q, Zhang KQ, Bioinhibitory effect of hydrogenotrophic bacteria on nitrate reduction by nanoscale zero-valent iron. *Chemosphere* **103**: 86–91 (2014).

26 Liu HF, Zheng BJ, Xu DD, Fu CY, Luo Y, Effect of sulfate-reducing bacteria and iron-oxidizing bacteria on the rate of corrosion of an aluminum alloy in a central air-conditioning cooling water system. *Ind Eng Chem Res* **53**: 7840–7846 (2014).

27 Wang H, Ju LK, Castaneda H, Cheng G, Newby BMZ, Corrosion of carbon steel C1010 in the presence of iron oxidizing bacteria *Acidithiobacillus ferrooxidans*. *Corros Sci* **89**: 250–257 (2014).

28 Liu HW, Gu TY, Zhang GA, Liu L, The effect of magneticfield on biomineralization and corrosionbehavior of carbon steel induced by iron-oxidizing bacteria. *Corros Sci* **102**: 93–102 (2016).

29 Solisio C, Lodi A, Converti A, Borghi MD, The effect of acid pre-treatment on the biosorption of Chromium(III) by *Sphaerotilus natans* from industrial wastewater. *Water Res* **34**: 3171– 3178 (2000).

30 Kondo K, Takeda M, Mashima T, Katahira M, Koizumi J, Ueda K, Conformational analysis of an extracellular polysaccharide produced by *Sphaerotilus natans*.

Carbohyd Res **360**: 102–108 (2012).

31 Starosvetsky J, Starosvetsky D, Pokroy B, Hilel T, Armon R, Electrochemical behaviour of stainless steels in media containing iron-oxidizing bacteria (IOB) by corrosion process modeling. *Corros Sci* **50**: 540–547 (2008).

32 Caravelli AH, Giannuzzi L, Zaritzky NE, Reduction of hexavalent chromium by *Sphaerotilus natans* a filamentous micro-organism present in activated sludges. *J Hazard Mater* **156**: 214–222 (2008).

33 APHA-AWWA-WEF, Standard methods for examination of water and wastewater, 20th ed. American Public Health Association, Washington, DC (1998).

34 Tang S, Wang XM, Mao YQ, Zhao Y, Yang HW, Xie YF, Effect of dissolved oxygen concentration on iron efficiency: Removal of three chloroacetic acids. *Water Res* **73**: 342–352 (2015).

35 Geng B, Jin ZH, Li TL, Qi XH, Kinetics of hexavalent chromium removal from water by chitosan-Fe^0 nanoparticles, *Chemosphere* **75**: 825–830 (2009).

36 Lefevre E, Bossa N, Wiesner MR, Gunsch CK, A review of the environmental implications of in situ remediation by nanoscale zero valent iron (nZVI): Behavior, transport and impacts on microbial communities. *Sci Total Environ* **565**: 889–901 (2016).

37 Zhang WX, Nanoscale iron particles for environmental remediation: an overview. *J Nanopart Res* **5**: 323-332 (2003).

38 Wilson SC, Lockwood PV, Ashley PM, Tighe M, The chemistry and behaviour of

antimony in the soil environment with comparisons to arsenic: a critical review, *Environ Pollut* **158**: 1169–1181 (2010).

39 Shi ZQ, Nurmi JT, Tratnyek PG, Effects of nano zero-valent iron on oxidation-reduction potential. *Environ Sci Technol* **45**: 1586–1592 (2011).

40 Yu RF, Chi FH, Cheng WP, Chang JC, Application of pH, ORP, and DO monitoring to evaluate chromium(VI) removal from wastewater by the nanoscale zero-valent iron (nZVI) process. *Chem Eng J* **255**: 568–576 (2014).

41 Yoon IH, Bang S, Chang JS, Kim MG, Kim KW, Effects of pH and dissolved oxygen on Cr(VI) removal in Fe(0)/H_2O systems. J Hazard Mater **186**: 855–862 (2011).

42 Beolchini F, Pagnanelli F, Toro L, Vegliò F, Ionic strength effect on copper biosorption by *Sphaerotilus natans*: equilibrium study and dynamic modelling in membrane reactor. *Water Res* **40**: 144–152 (2006).

43 Qin YC, Guan XH, Wang HT, Sorption of Cu^{2+} by *Sphaeotilus natans* and its biosorption mechanism. *Acta Scientiae Circumstantiae* **28**: 892–896 (2008).

44 Wu HY, Chen WL, Rong XM, Cai P, Dai K, Huang QY, Adhesion to kaolinite and goethite of *Pseudomonas putida* at different growth phases. *Chem Geol* **390**: 1–8 (2014).

45 Nghiem LD, Manassa P, Dawson M, Fitzgerald SK, Oxidation reduction potential as a parameter to regulate micro-oxygen injection into anaerobic digester for reducing hydrogen sulphide concentration in biogas. *Bioresource Technol* **173**: 443–447

(2014).

46 Bazrafshan H, Tesieh ZA, Dabirnia S, Touba RS, Manghabati H, Nasernejad B, Synthesis of novel α-Fe_2O_3 nanorods without surfactant and its electrochemical performance. *Powder Technol* **308**: 266–272 (2017).

47 Sheng JP, Baikenov MI, Liang XY, Rao XH, Ma FY, Su XT, Zhang Y, Rapid separation and large-scale synthesis of β-FeOOH nanospindles for direct coal liquefaction. *Fuel Process Technol* **165**: 80–86 (2017).

48 Wan CC, Jiao Y, Qiang TG, Li J, Cellulose-derived carbon aerogels supported goethite (α-FeOOH) nanoneedles and nanoflowers for electromagnetic interference shielding. *Carbohyd Polym* **156**: 427–434 (2017).

49 Chen YY, Furmann A, Mastalerz M, Schimmelmann A, Quantitative analysis of shales by KBr-FTIR and micro-FTIR. *Fuel* **116**: 538–549 (2014).

50 Shen L, Ziheng J, Wang D, Wang YP, Lu YH, Enhance wastewater biological treatment through the bacteria induced graphene oxide hydrogel. *Chemosphere* **190**: 201-210 (2017).

51 Li CY, Wang S, Du XP, Cheng XS, Fu M, Hou N, Li DP, Immobilization of iron- and manganese-oxidizing bacteria with a biofilm-forming bacterium for the effective removal of iron and manganese from groundwater. *Bioresource Technol* **220**: 76–84 (2016).

52 Sun Zhenya. Characterization and self-assembly synthesis of biomineralized nano-FeOOH and its environmental significance (Doctoral thesis). Wuhan: Wuhan

University of Technology, 2006. in Chinese

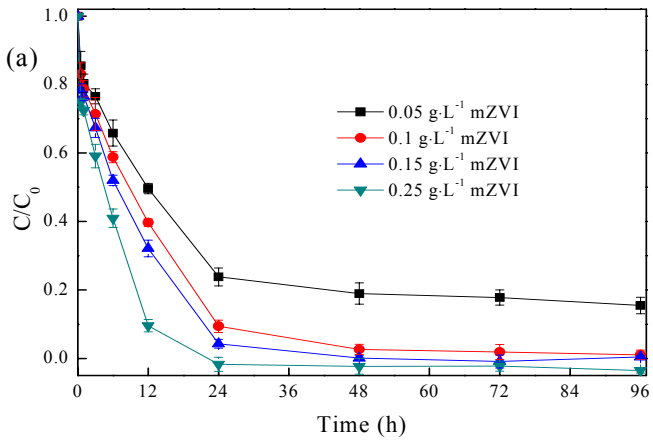

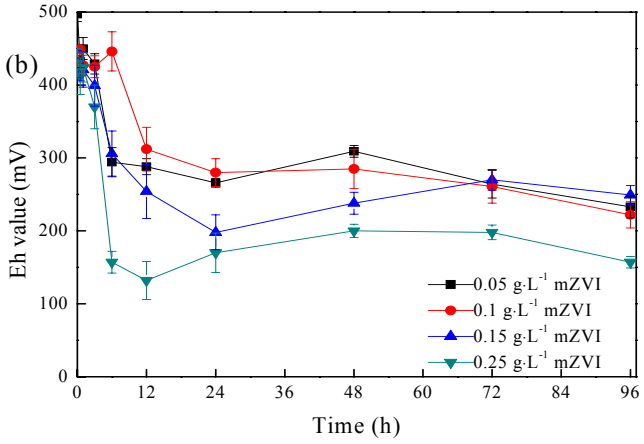

Figure 1. (a) ZVI adsorption ability towards Sb(V) in solution without purging with N_2, and (b) the corresponding Eh value in solution as the reaction progressed.

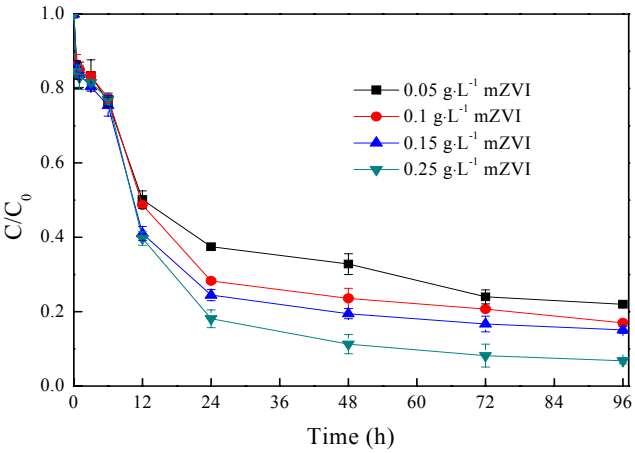

Figure 2. mZVI adsorption ability towards Sb(V) in solution after being purged with N_2.

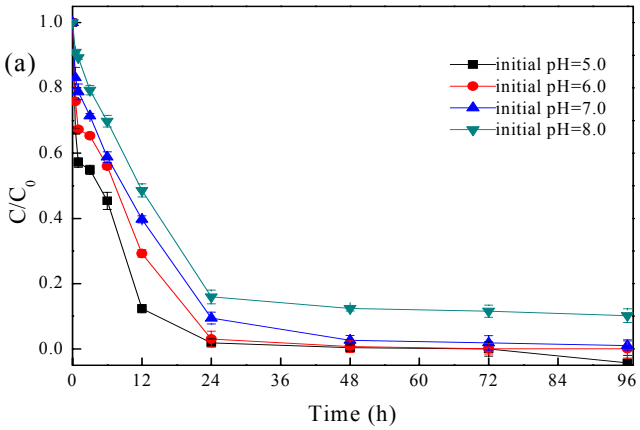

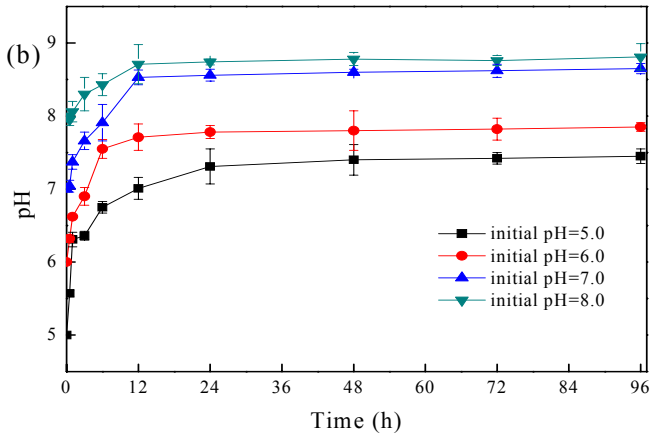

Figure 3. (a) Removal of Sb(V) from water with ZVI at different initial pH, and (b) variation of pH values as the reaction progressed.

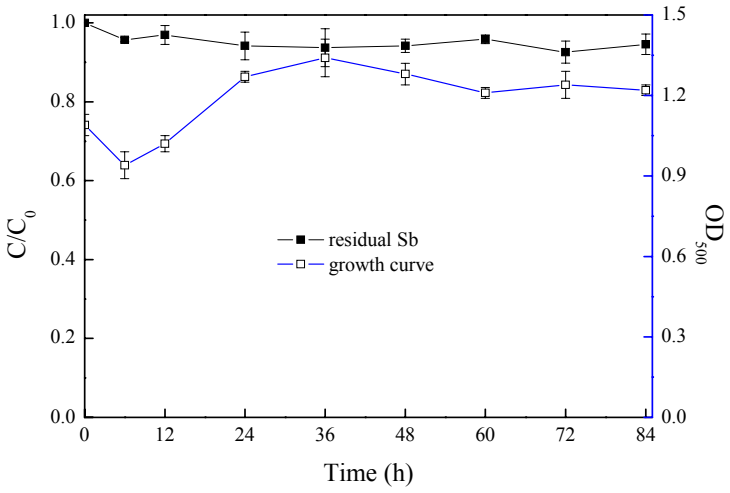

Figure 4. Bioadsorption ability of *Sphaerotilus natans* and its growth performance in Sb(V) solution.

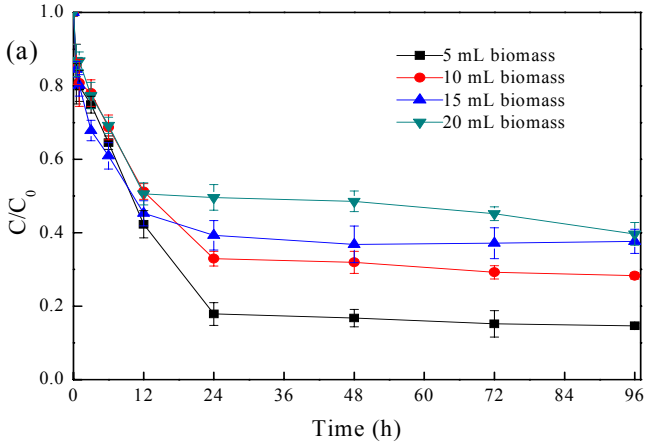

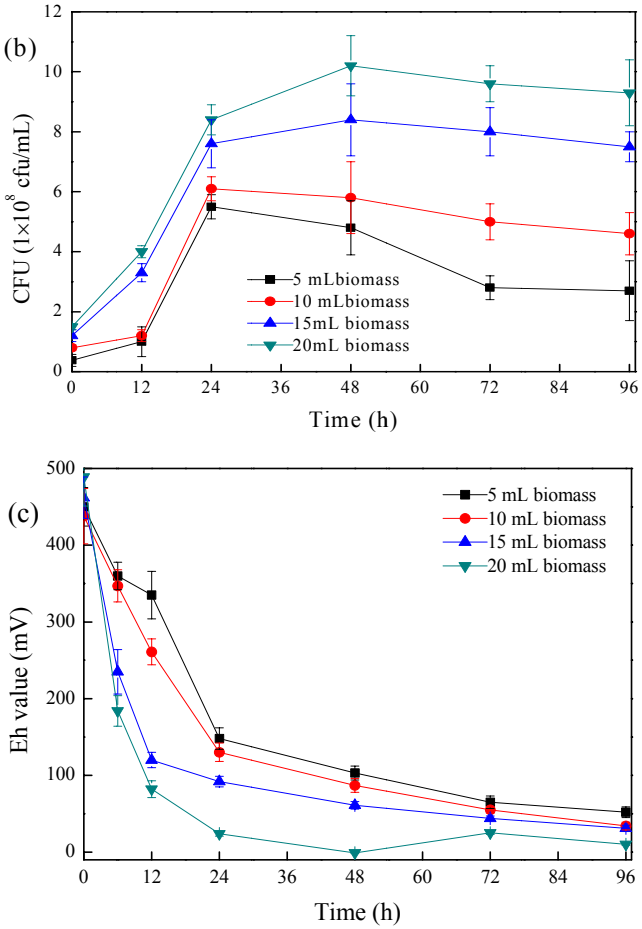

Figure 5. (a) Sb(V) removal of ZVI in the presence of *Sphaerotilus natans*, and changes of (b) the number of CFU and (c) Eh value in solution as the reaction progressed.

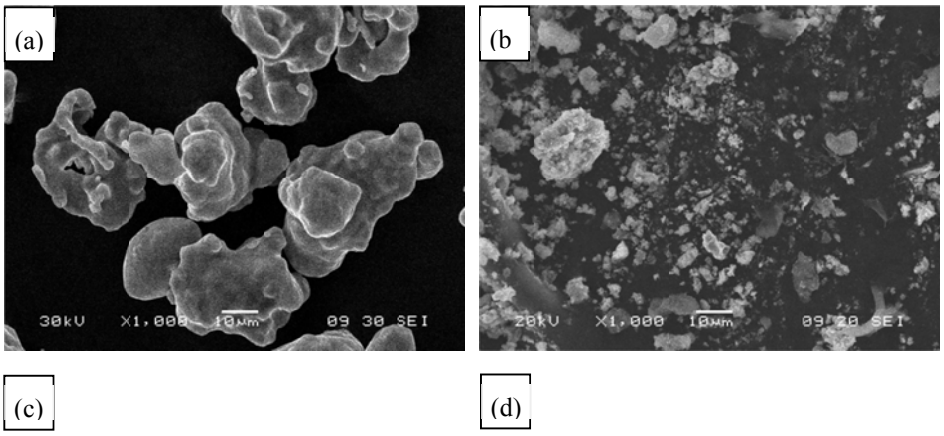

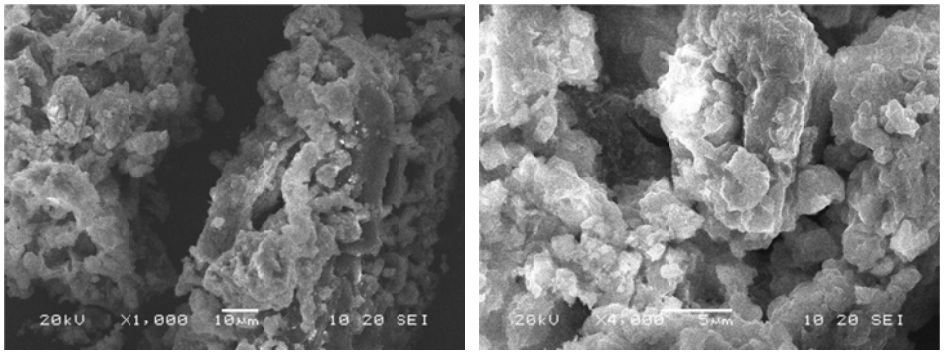

Figure 6. SEM images of (a) mZVI before reaction, (b) generated precipitate from reaction system without the presence of *Sphaerotilus natans*, and (c, d) product from reaction system with the presence of *Sphaerotilus natans*.

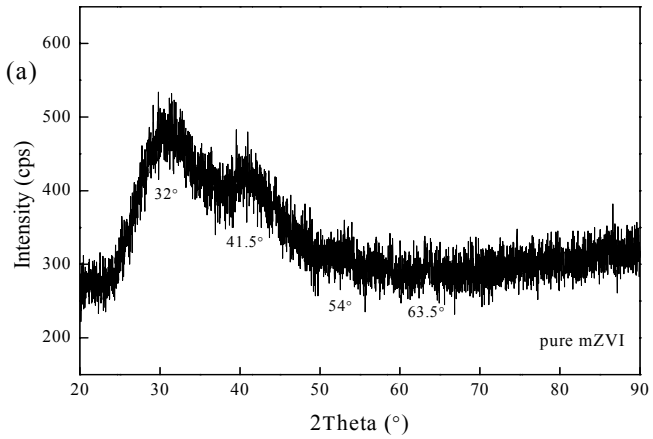

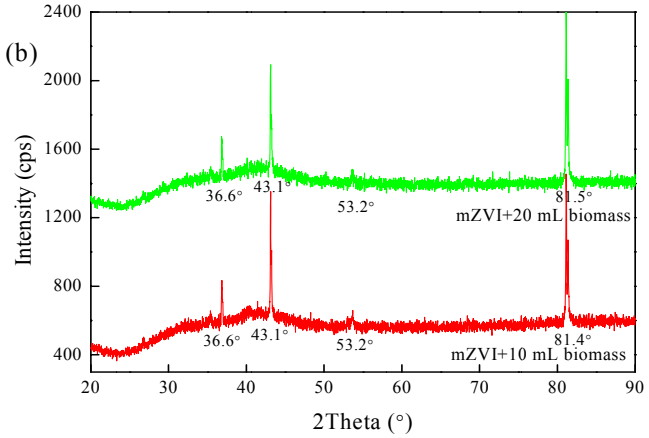

Figure 7 XRD patterns of product obtained from (a) the abiotic system and (b) biological system.

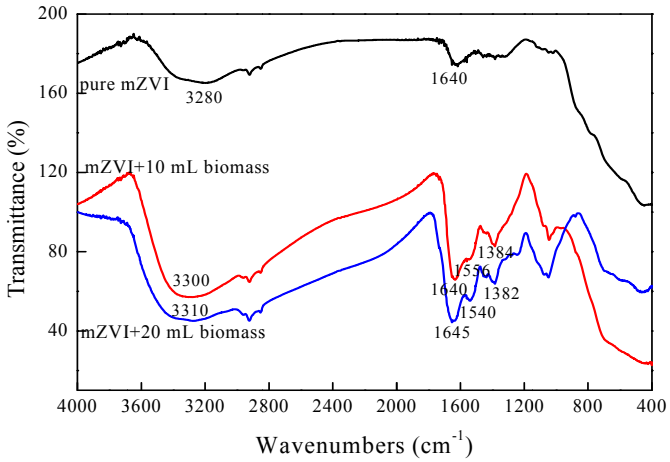

Figure 8. FTIR spectra of product obtained from the abiotic and biological system.

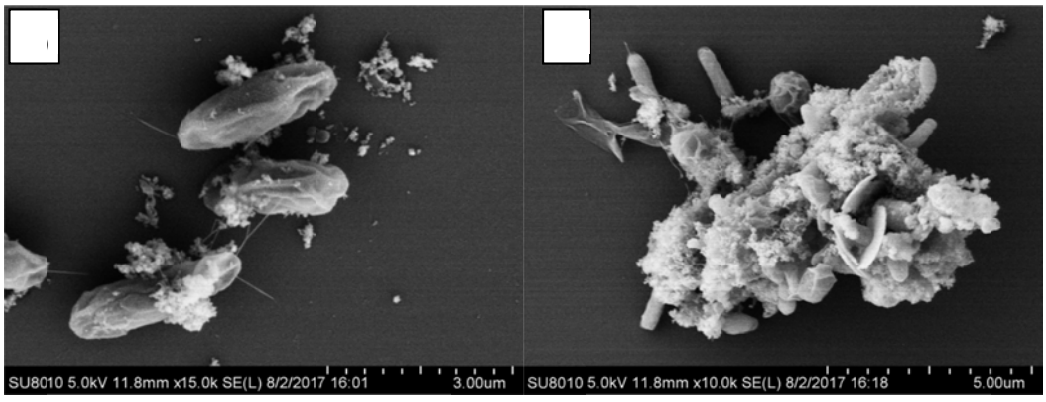

Figure 9. (a, b) HRSEM images of *Sphaerotilus natans* in biological system after reaction.

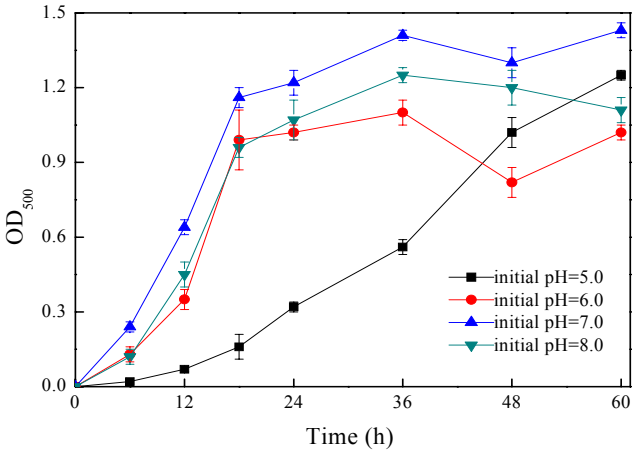

Figure S1 Growth curve of *Sphaerotilus natans* at different starting pH values.